

## Nuclear $\gamma$ -Tubulin during Acentriolar Plant Mitosis

Pavla Binarová,<sup>a,1</sup> Věra Cenková,<sup>b</sup> Bettina Hause,<sup>c</sup> Elena Kubátová,<sup>a</sup> Martin Lysák,<sup>b</sup>  
Jaroslav Doležel,<sup>b</sup> László Bögre,<sup>d</sup> and Pavel Dráber<sup>e</sup>

<sup>a</sup> Institute of Microbiology, Academy of Sciences of the Czech Republic, Vídeňská 1083, 142 20 Prague 4, Czech Republic

<sup>b</sup> Institute of Experimental Botany, Academy of Sciences of the Czech Republic, Sokolovská 6, 772 00 Olomouc, Czech Republic

<sup>c</sup> Institute of Plant Biochemistry, P.O. Box 110432, D-06018 Halle, Germany

<sup>d</sup> School of Biological Sciences, Royal Holloway, University of London, Surrey, United Kingdom

<sup>e</sup> Institute of Molecular Genetics, Academy of Sciences of the Czech Republic, Vídeňská 1083, 142 20 Prague 4, Czech Republic

Neither the molecular mechanism by which plant microtubules nucleate in the cytoplasm nor the organization of plant mitotic spindles, which lack centrosomes, is well understood. Here, using immunolocalization and cell fractionation techniques, we provide evidence that  $\gamma$ -tubulin, a universal component of microtubule organizing centers, is present in both the cytoplasm and the nucleus of plant cells. The amount of  $\gamma$ -tubulin in nuclei increased during the G<sub>2</sub> phase, when cells are synchronized or sorted for particular phases of the cell cycle.  $\gamma$ -Tubulin appeared on prekinetochores before preprophase arrest caused by inhibition of the cyclin-dependent kinase and before prekinetochore labeling of the mitosis-specific phosphoepitope MPM2. The association of nuclear  $\gamma$ -tubulin with chromatin displayed moderately strong affinity, as shown by its release after DNase treatment and by using extraction experiments. Subcellular compartmentalization of  $\gamma$ -tubulin might be an important factor in the organization of plant-specific microtubule arrays and acentriolar mitotic spindles.

### INTRODUCTION

Microtubules are formed by the polymeric self-organization of tubulin. This process is initiated at microtubule organizing centers (MTOCs). In plants, different microtubular arrays, such as interphase cortical microtubules and the preprophase bands, perinuclear microtubules, mitotic spindles, and phragmoplasts, are dynamically formed at distinct locations and interchanged during the cell cycle. Discrete MTOCs, comparable to centrosomes in animals, are not known in plants; rather, the concept of microtubule nucleation sites dispersed throughout the plant cell has been proposed by Mazia (1984). Microtubules can nucleate on noncentrosome-dependent sites, even in cells possessing centrosomes (Heald et al., 1997; Vorobjev et al., 1997; Yvon and Wadsworth, 1997), but the contribution of different forms of microtubule nucleation sites in generating the microtubule pattern is not known (Hyman and Karsenti, 1998).

In mitotic cells of vertebrates, the chromosomes capture and stabilize the microtubules nucleated by the centrosomes but do not appear to stimulate microtubule growth (Zhang and Nicklas, 1995). On the other hand, in acentriolar

systems, such as *Drosophila* during male meiosis or in parthenogenic *Sciara* embryos, the chromosomes act as MTOCs (Bonnacorsi et al., 1998; De Saint Phalle and Sullivan, 1998). Current models of spindle formation in the absence of centrioles are based on chromatin-mediated microtubule organization and the ability of microtubule-associated molecular motors to focus microtubules into polar arrays (Heald et al., 1996, 1997; Karpen and Endow, 1998).

In plant meiocytes, microtubules initially were found to appear around the prometaphase chromosomes, indicating a chromatin-mediated spindle assembly mechanism similar to that described for animal meiocytes (Chan and Cande, 1998). In plant mitosis, which is acentriolar as well, the nuclear envelope was shown to be an important site for microtubule nucleation during the late G<sub>2</sub> stage of the cell cycle (Stoppin et al., 1996). After the breakdown of the nuclear envelope, the metaphase spindle is formed predominantly by kinetochore fibers (Palevitz, 1993; Smirnova and Bajer, 1998). How the putative microtubule organizing sites, which are dispersed throughout the cytoplasm, on the nuclear envelope, or at the chromosomes, participate in plant spindle organization is not clear.

To understand plant microtubule organization, one first must identify the molecular composition of the dispersed microtubule nucleation sites. In animals and fungi,  $\gamma$ -tubulin

<sup>1</sup> To whom correspondence should be addressed. E-mail binarova@biomed.cas.cz; fax 420-2-4752384.

has been detected at all MTOCs, in which it is suggested to nucleate and organize microtubules (Oakley et al., 1990; Joshi et al., 1992).  $\gamma$ -Tubulin is a part of numerous complexes of various sizes and composition (Jeng and Stearns, 1999), such as those identified in *Xenopus* eggs extracts (Zheng et al., 1995), somatic cells of mammals (Stearns and Kirschner, 1994; Moudjou et al., 1996), *Aspergillus nidulans* (Akashi et al., 1997), yeast (Knop and Schiebel, 1997), and *Drosophila* (Moritz et al., 1998; Oegema et al., 1999). Some studies indicate a possible involvement of cytoplasmic  $\gamma$ -tubulin in nucleation or stabilization (or both) of the minus ends of noncentrosomal microtubules (Kube-Granderath and Schliwa, 1997; Yvon and Wadsworth, 1997). Although no experimental data are available proving the role of  $\gamma$ -tubulin in chromatin-controlled microtubule nucleation, its involvement has been postulated (Hyman and Karsenti, 1998). In plant cells,  $\gamma$ -tubulin is located along all microtubular arrays (Liu et al., 1993, 1995; Joshi and Palevitz, 1996) and on kinetochores of isolated plant chromosomes (Binarová et al., 1998a).

Here, we report the presence of nuclear and cytoplasmic  $\gamma$ -tubulin forms in plant cells. Accumulation of a nuclear  $\gamma$ -tubulin pool during the  $G_2$  phase of the cell cycle indicates its involvement in the modulation or stabilization of chromosome-microtubule interactions, which are important but poorly understood events in formation of acentriolar plant cell spindles.

## RESULTS

### $\gamma$ -Tubulin Localization in Nuclei

$\gamma$ -Tubulin was immunolocalized along all microtubular arrays by using monoclonal antibodies TU-30, TU-31, and TU-32, which are directed against the C-terminal region of the  $\gamma$ -tubulin molecule. Not only were the cortical microtubules, the preprophase band, the mitotic spindle, and the phragmoplast labeled, but discrete staining was found in some interphase nuclei (Figures 1A and 1B). Preabsorbing the antibodies with the peptide used for immunization prevented the immunostaining. To analyze whether  $\gamma$ -tubulin was present in interphase nuclei at a particular stage of the cell cycle, we processed synchronized root tip cells for immunolabeling. No distinct staining of  $\gamma$ -tubulin was observed in nuclei during the  $G_1$  stage of the cell cycle (Figures 1C and 1D). From the early  $G_2$  phase on, however,  $\gamma$ -tubulin appeared in the nuclei as discrete spots, gradually increasing in size until the late  $G_2$  stage, when they often were seen as double spots (Figures 1E and 1F). A similar spotty labeling pattern for  $\gamma$ -tubulin was found in isolated  $G_2$  nuclei (Figures 2G and 2H). When the cells progressed to mitosis,  $\gamma$ -tubulin labeling decorated the kinetochore microtubules of the mitotic spindle (Figures 1A and 1B) and was associated with the kinetochore region of isolated chromosomes (Figures 1I and 1J).

$\gamma$ -Tubulin spots more often were localized closer to the nuclear periphery than to the center of nuclei, as revealed by three-dimensional reconstruction of images from double labeling of  $G_2$  nuclei with the anti- $\gamma$ -tubulin antibody and the DNA binding dye 4',6-diamidino-2-phenylindole (DAPI). A typical staining pattern is shown as stereopairs in Figure 2A. Optical sectioning of  $G_2$  nuclei confirmed that the  $\gamma$ -tubulin spots were inside the nuclei, adjacent to the chromatin. However,  $\gamma$ -tubulin also was found on the nuclear surface, decorating perinuclear microtubules that were focused to the poles, as documented on 12 consecutive sections in Figure 2B. The number of spots and double spots per nucleus varied from one to eight. Spots of  $\gamma$ -tubulin apparently were located in the prekinetochore region, but the  $\gamma$ -tubulin signal also was found at other locations within the nucleus, namely, in the vicinity of condensing chromatin. Short fibers originating from kinetochores and decorated with  $\gamma$ -tubulin antibody occasionally could be observed during the late prophase (Figure 2E). Antibodies recognizing abundant nuclear proteins, such as the nucleolin or the mitogen-activated protein kinase MMK1, failed to stain the prekinetochores but did label nucleoli and nucleoplasm, respectively (data not shown).

The mitosis-specific MPM2 phosphoepitope has been established as a marker for prekinetochores in nuclei in the late  $G_2$  stage (Binarová et al., 1993). Therefore, we compared the timing and location of the  $\gamma$ -tubulin staining and the prekinetochore labeling with MPM2. In synchronously dividing root meristem cells,  $\gamma$ -tubulin was detected earlier in  $G_2$ -stage nuclei than the MPM-2 phosphoepitope. To dissect the timing of  $\gamma$ -tubulin appearance on kinetochores, we further synchronized the root tip cells by arresting them during late  $G_2$  stage with a low dose of the cyclin-dependent kinase inhibitor roscovitine, as described previously (Binarová et al., 1998b). In the presence of roscovitine, cells were arrested during  $G_2$  phase with condensed chromosomes surrounded by persistent nuclear envelopes observed by phase-contrast microscopy. Labeled  $\gamma$ -tubulin was visible in the kinetochore region of the condensed chromosomes (Figure 2C), which is a pattern similar to the kinetochore labeling obtained with the MPM2 antibody (Figure 2D). The MPM2 phosphoepitope, but not  $\gamma$ -tubulin, also was present in the nucleoplasm (Figures 2C and 2D).

$\gamma$ -Tubulin spots remained visible in  $G_2$  nuclei if the microtubular cytoskeleton was depolymerized with the antimicrotubular drug amiprophos-methyl (APM) or stabilized with taxol (data not shown). Nuclear labeling of  $\gamma$ -tubulin also was observed in several other plant species, for example, pea and alfalfa (data not shown).

The antibodies against  $\gamma$ -tubulin recognized a single band of 58 kD during immunoblot analysis; no cross-reactivity with other proteins in the cell extracts was detected (Figure 3A). Preincubating the antibodies with the peptide used for immunization abolished immunostaining reactions. Densitometric analyses of immunoblots showed that ~70% from the total  $\gamma$ -tubulin pool remained in the supernatant after centrifugation of the cell extract. Similarly, 70% of the total

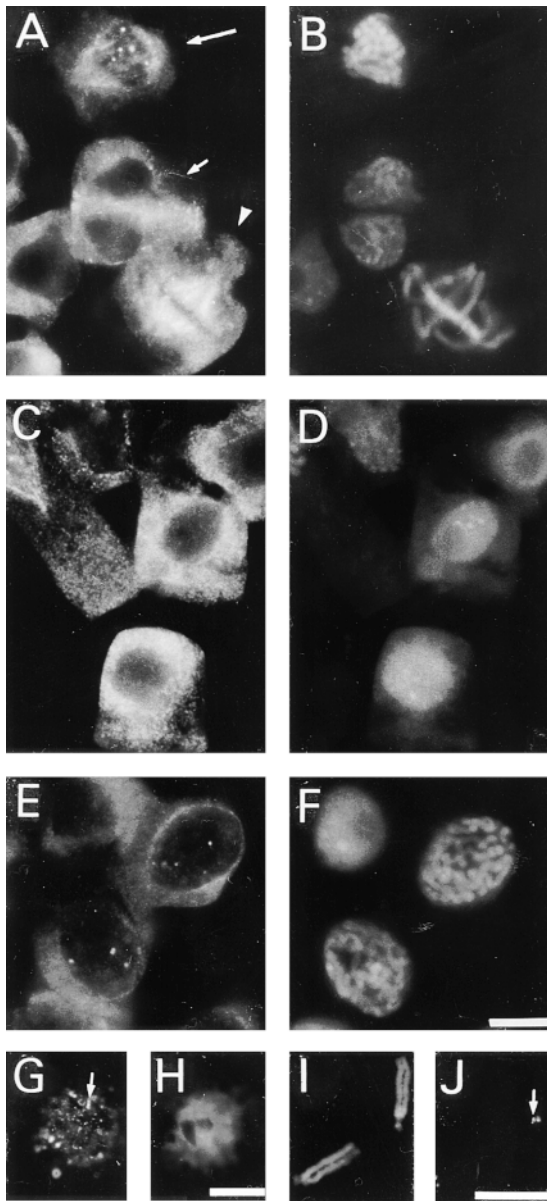


**Figure 1.** Immunolocalization of  $\gamma$ -Tubulin in Fava Bean Cells, Isolated Nuclei, and Isolated Chromosomes.

$\gamma$ -Tubulin staining [(A), (C), (E), (G), and (J)] and corresponding chromatin labeling with DAPI [(B), (D), (F), (H), and (I)].

(A) and (B) Group of cells in different stages of the cell cycle. Staining of  $\gamma$ -tubulin in prophase nuclei (long arrow in [A]), in metaphase spindle (arrowhead in [A]), and in telophase phragmoplast (short arrow in [A]).

(C) and (D) Cells during the  $G_1$  stage of the cell cycle.

(E) and (F) Cells in the late  $G_2$  stage of the cell cycle with staining of  $\gamma$ -tubulin in nuclei.

(G) and (H) Isolated  $G_2$  nuclei with  $\gamma$ -tubulin staining (arrow in [G]).

(I) and (J) Isolated chromosomes with staining of  $\gamma$ -tubulin in the kinetochore region (arrow in [J]).

Bar in (F) = 10  $\mu$ m for (A) to (F); bar in (H) = 10  $\mu$ m for (G) and (H); bar in (J) = 10  $\mu$ m for (I) and (J).

$\alpha$ - and  $\beta$ -tubulins present were detected in the supernatant (Figure 3A).

The existence of a nuclear  $\gamma$ -tubulin pool was further confirmed by immunoblot analysis with purified nuclei (Figure 3B, lane 1). To determine the nature of  $\gamma$ -tubulin association with nuclear structures, we extracted the nuclei by using buffers containing various salt concentrations or chaotropic agents or subjected the nuclei to DNase treatment. As shown in Figure 3B (lanes 3 and 4),  $\gamma$ -tubulin was not extracted by 75 mM NaCl. Increasing the salt concentration to 200 mM extracted  $\sim$ 50% of the  $\gamma$ -tubulin from the nuclei (Figure 3B, lanes 5 and 6), and further increasing the salt concentration to 300 mM extracted all  $\gamma$ -tubulin from the nuclei. All  $\gamma$ -tubulin was removed from isolated nuclei by extraction with 0.5 M KI (Figure 3B, lanes 7 and 8), 4 M urea, or 0.5% deoxycholate plus 0.1% SDS (data not shown). When treated with DNase,  $\gamma$ -tubulin was released from the nuclei along with DNA (Figure 3C, lanes 2 and 3). In control samples treated under identical conditions but without DNase,  $\gamma$ -tubulin was found mainly in the pelleted nuclei fraction (Figure 3C, lanes 4 and 5).

#### Changes in Nuclear $\gamma$ -Tubulin during the Cell Cycle

Because the immunofluorescence results indicated an accumulation of  $\gamma$ -tubulin during the  $G_2$  stage of the cell cycle, we used flow cytometry to separate nuclei that were in the  $G_1$  or  $G_2$  stage and then analyzed them further. Aside from separating and collecting nuclei in various particular stages of the cell cycle, this separation technique eliminated any possible cytoplasmic contamination of nuclear samples, which could occur if the nuclei were isolated only by using a sucrose gradient. A DNA content histogram used to assess the results of sorting nuclei during the  $G_2$  stage from synchronized root meristem cells is shown in Figure 4A. Only the nuclei sorted in the R1 area of the dot plot graph were used for further analysis. The purity of the samples also could be determined by the characteristic morphology of the nuclei in  $G_1$  or  $G_2$  phases, stained by DAPI, as shown in Figure 4B. For comparison, the same numbers of nuclei in the two particular cell cycle stages were immunoblotted. Densitometry of the blots showed that the  $G_2$  nuclei contained  $\sim$ 50% more  $\gamma$ -tubulin than did the  $G_1$  nuclei (Figure 4C). In contrast, the cytosolic fractions of cells in the  $G_1$  and  $G_2$  stages did not differ in the amount of  $\gamma$ -tubulin present (Figure 4D).

#### DISCUSSION

The finding of plant homologs to  $\gamma$ -tubulin, which is suggested to universally nucleate microtubules in MTOCs in eukaryotes (Oakley et al., 1990; Joshi et al., 1992), provides the most plausible molecular component for microtubule nucleation in plant cells. However, immunolocalization studies

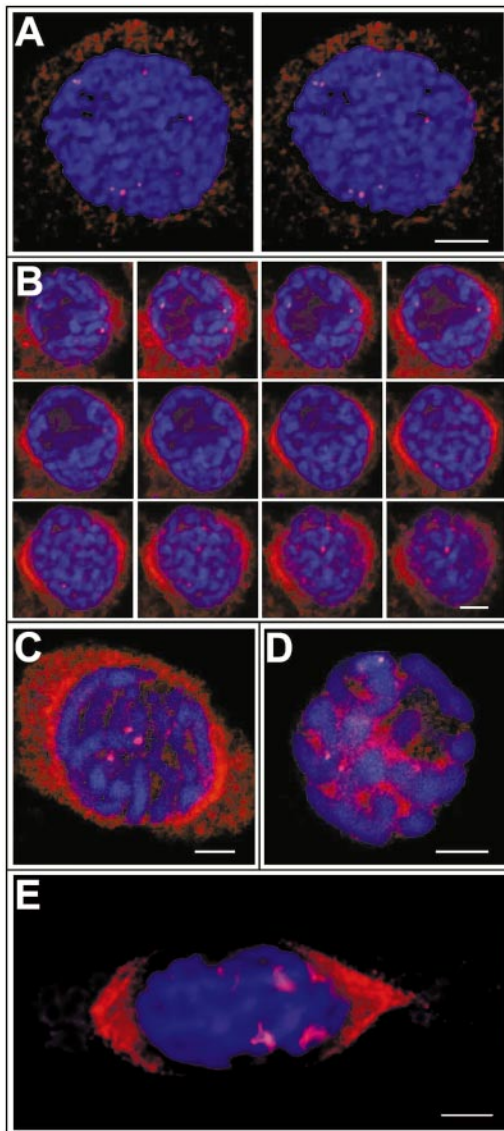


**Figure 2.** Confocal Scanning Laser Microscopy of DNA,  $\gamma$ -Tubulin, and MPM2 Staining of Fava Bean Meristem Cells.

Optical sections  $1.0\ \mu\text{m}^2$  thick exhibit  $\gamma$ -tubulin labeling (red) and DNA staining (blue).

**(A)** Stereopair of a cell in early  $G_2$  stage of the cell cycle; stereomages were obtained by progression through a three-dimensional reconstruction program.

**(B)** Gallery of 12 optical sections of a cell in late  $G_2$  stage of the cell cycle. Note that some of the  $\gamma$ -tubulin-labeled dots are located at the chromosomes near the nuclear envelope, and perinuclear  $\gamma$ -tubulin forms caps that are focused to the poles.

**(C)** Optical section through a roscovitine-treated cell showing the distribution of  $\gamma$ -tubulin.

**(D)** Optical section through a roscovitine-treated cell showing the distribution of the MPM2 antigen. Note that the MPM2 signal is associated with the kinetochore/centromeric region and is also seen in the nucleoplasm, whereas  $\gamma$ -tubulin is restricted to the kinetochore/centromeric region.

have been unable to directly confirm the role of  $\gamma$ -tubulin in microtubule nucleation, because  $\gamma$ -tubulin is not found at discrete sites but instead is distributed along all microtubular arrays as well as at the kinetochore region of isolated chromosomes (Liu et al., 1995; Binarová et al., 1998a). Therefore, we decided to complement the immunolocalization studies with biochemical characterization of  $\gamma$ -tubulin in subcellular fractions at various points in the cell cycle.

Most of the  $\gamma$ -tubulin was detected in the cytoplasm after cell fractionation, but in agreement with the immunolocalization data, a small portion ( $\sim 0.1\%$  of the total  $\gamma$ -tubulin pool) was found in the nuclear fraction. The presence of  $\gamma$ -tubulin in plant nuclei is unexpected, because nuclear  $\gamma$ -tubulin has been described only in organisms with intranuclear mitosis, such as fungi (Akashi et al., 1997; Knop and Schiebel, 1997) or protists (Curtenaz et al., 1997). Previously, we found  $\gamma$ -tubulin to be associated with the kinetochore/centromeric region of plant chromosomes in cells after treatment with antimicrotubular drugs and on isolated chromosomes (Binarová et al., 1998a, 1998b). Perhaps in those experiments, the  $\gamma$ -tubulin relocated to the kinetochore during the treatment with antimicrotubular drugs used for metaphase accumulation, before the chromosomes were isolated. Here, we found  $\gamma$ -tubulin in premitotic nuclei in cells that had not undergone treatment with antimicrotubular drugs. Associated mainly with the region corresponding to prekinetochores,  $\gamma$ -tubulin also could be detected at other sites of the chromosome arms.  $\gamma$ -Tubulin is retained in the nucleus by chromatin, as shown by its release by DNase treatments. Its binding to chromatin is moderately strong, being solubilized only at salt concentrations  $>250\ \text{mM}$ , and the binding does not appear to depend on intact microtubules, as suggested by the presence of  $\gamma$ -tubulin on kinetochores in cells treated with antimicrotubular drugs.

Previous experiments with polyclonal or monoclonal antibodies directed against the N-terminal part of the  $\gamma$ -tubulin molecule failed to detect  $\gamma$ -tubulin in nuclei (Liu et al., 1993, 1995; McDonald et al., 1993). Similarly, when we stained fava bean meristem cells or isolated chromosomes with N-terminal  $\gamma$ -tubulin antibodies, only the microtubule arrays were decorated, and no staining was observed in the nuclei (P. Binarová, unpublished data). We believe that the observed differences in the staining pattern with antibodies raised against different  $\gamma$ -tubulin regions reflect either a specific orientation or a masking of  $\gamma$ -tubulin molecules in assembled microtubules or associated with chromatin. Differences in the exposure of C- and N-terminal tubulin domains in cytoplasmic microtubules also have been described for animal (Dráber et al., 1989) and plant (Smertenko et al., 1997) cells.

**(E)** Cell with prophase spindle and short kinetochore fibers decorated with anti- $\gamma$ -tubulin antibody.

Bars in **(A)** to **(E)** =  $5\ \mu\text{m}$ .

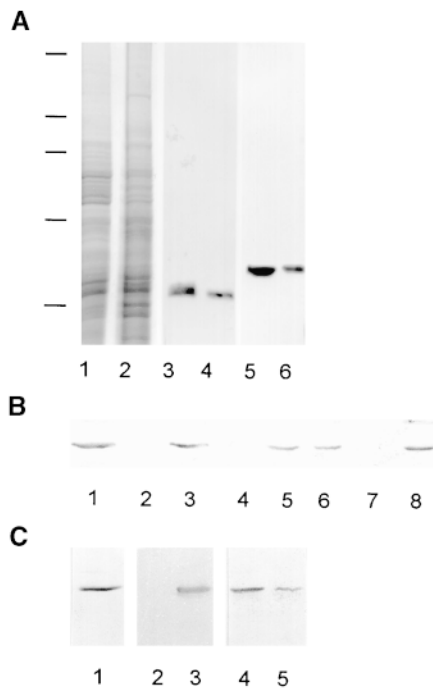


**Figure 3.**  $\gamma$ -Tubulin in Cellular Fractions of Asynchronous Meristem Root Tips of Fava Bean.

**(A)** Protein gel blot analysis of supernatant (lanes 1, 3, and 5) and pellet (lanes 2, 4, and 6) of centrifuged cell extracts. Shown are Coomassie blue staining (lanes 1 and 2) and immunostaining with antibodies raised against  $\alpha$ -tubulin (lanes 3 and 4) or against  $\gamma$ -tubulin (lanes 5 and 6). Positions of molecular mass standards are indicated at left by horizontal lines (from top to bottom: 205, 116, 97, 66, and 45 kD). Each lane was loaded with 10  $\mu$ g of protein.

**(B)** Solubilization of nuclear  $\gamma$ -tubulin under various buffer conditions. Isolated nuclei were treated in suspension and then pelleted by centrifugation. Pelleted nuclei (lanes 1, 3, 5, and 7) and supernatants (lanes 2, 4, 6, and 8) were used for protein gel blot analysis. Nuclei and the supernatant of the control were treated with buffer only (lanes 1 and 2), 75 mM NaCl (lanes 3 and 4), 200 mM NaCl (lanes 5 and 6), or 0.5 M KI (lanes 7 and 8).

**(C)** Treatment of isolated nuclei with DNase. Shown are the results of protein gel blot analysis of untreated nuclei (lane 1), pelleted nuclei after DNase treatment (lane 2), supernatant after DNase treatment (lane 3), control pelleted nuclei (lane 4), and control supernatant (lane 5). Proteins from 200,000 nuclei were loaded per lane.

Chromatin-mediated microtubule organization is the basic mechanism of spindle formation in animal and plant meicytes lacking centrosomes (Chan and Cande, 1998; reviewed in Karpen and Endow, 1998). Our studies of  $\gamma$ -tubulin localization in plant meicytes indicate a colocalization with all microtubular arrays. Although  $\gamma$ -tubulin was not associated specifically with kinetochores of meicytes in prophase, it did colocalize with microtubules newly formed or captured in the vicinity of chromosomes (P. Binarová, un-

published data). Microtubule assembly in the vicinity of chromosomes is not restricted to meicytes; it also occurs in mitotic plant cells (Bajer and Ostergren, 1961; Binarová et al., 1998b; Smirnova and Bajer, 1998). Moreover, in both plant mitotic and animal meiotic cells, bipolar spindle-like structures can form in the cytoplasm in the absence of chromatin and centrosomes (Bajer and Mole-Bajer, 1986; Brunet et al., 1998). Thus, spindle formation appears to be an intrinsic property of the microtubules with their associated factors, with centrosomes or chromosomes perhaps only modulating this process. In plants, formation of the preprophase spindle by self-assembly in the cytoplasm surrounding the nuclear envelope is later followed and reinforced through chromosome (kinetochore)-mediated spindle assembly (Smirnova and Bajer, 1998). During the transition from  $G_2$  to M phase, just at a time of nuclear envelope breakdown, we found  $\gamma$ -tubulin in some of the short kinetochore microtubule fibers, indicating that at this point of spindle formation, kinetochore-located  $\gamma$ -tubulin interacts with captured preexisting microtubules or with newly formed ones. The specific timing of  $\gamma$ -tubulin appearance in  $G_2$  nuclei and its presence on kinetochores in prophase-arrested cells indicate an active transport mechanism into the nucleus. In yeast, the  $\gamma$ -tubulin complexes are assembled in the cytoplasm; their import into nuclei then is regulated by a cell cycle-dependent phosphorylation event of the nuclear localization sequence in Spc98 (Pereira et al., 1998). We found a considerably larger cytoplasmic pool of soluble  $\gamma$ -tubulin in plants than has been reported for animal cells (Stearns and Kirschner, 1994; Moudjou et al., 1996). In the soluble cytoplasmic pool,  $\gamma$ -tubulin was present in large and small protein complexes (P. Binarová, unpublished data). Given that soluble factors of unknown molecular composition from tobacco extracts are able to restore the nucleation activity of inactivated mammalian centrosomes (Stoppin-Mellet et al., 1999), we consider  $\gamma$ -tubulin complexes to be plausible candidates for such factors.

The molecular composition of kinetochores and the mechanisms of kinetochore-microtubule binding in yeast and animal cells are beginning to be understood (Sullivan, 1998). The maize homologs of MAD2 and CENPC are the first kinetochore proteins to have been molecularly characterized in plants (Dawe et al., 1999; Yu et al., 1999). Some antibodies raised against the animal centrosomal or kinetochore antigens recognize the plant proteins on prekinetochores during late interphase and during mitosis (Binarová et al., 1993; Houben et al., 1995; Yu et al., 1999). The MPM2 phosphoepitope labeling in the kinetochore/centromeric region from prophase to the end of metaphase provides a molecular marker for timing the appearance of  $\gamma$ -tubulin (Binarová et al., 1993).  $\gamma$ -Tubulin and MPM2 labeling colocalized in the kinetochore region only during later stages of  $G_2$  (around prophase) and in prophase-arrested cells; thus,  $\gamma$ -tubulin appears on kinetochores during the  $G_2$  phase, before the MPM2 phosphoepitope is generated.

The presence of  $\gamma$ -tubulin in kinetochores and its possible participation in nucleation of kinetochore microtubules are in

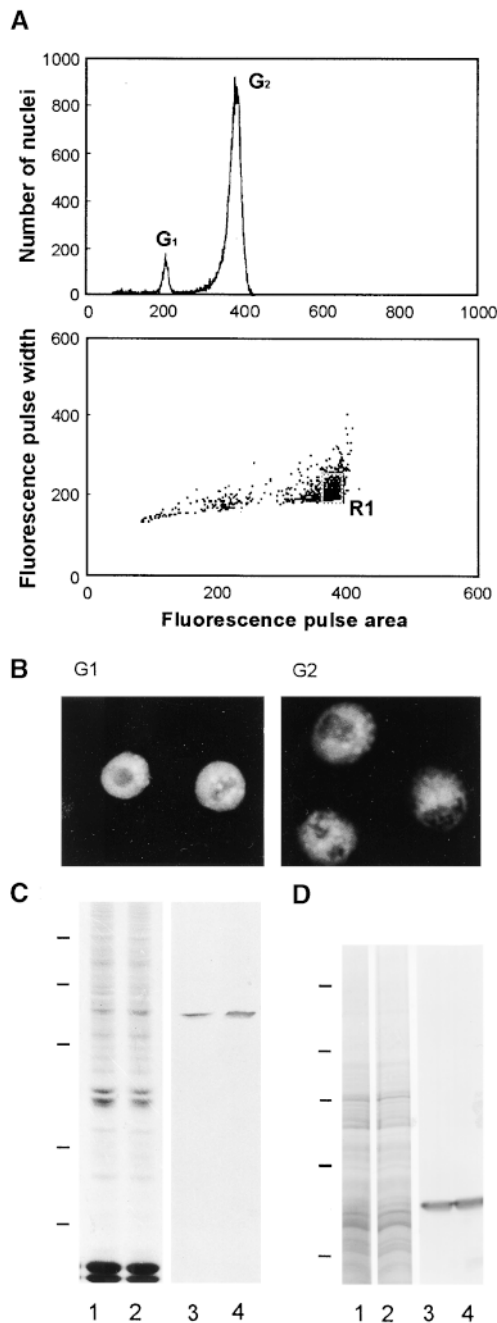


**Figure 4.** Flow Cytometric Sorting of Nuclei and Detection of  $\gamma$ -Tubulin during  $G_1$  and  $G_2$  Stages of the Cell Cycle.

**(A)** Example of flow sorting of synchronized  $G_2$  nuclei. At top is a histogram of relative fluorescence (fluorescence pulse area) derived after analysis of isolated nuclei, which shows a high degree of synchronization (high number of nuclei in  $G_2$  stage). At bottom is a dot plot of fluorescence pulse area versus fluorescence pulse width used for the sorting of nuclei. The population of  $G_2$  nuclei was sorted from the marked sort region (R1). Similarly, synchronized  $G_1$  nuclei were flow sorted.

contrast to the search-and-capture model of somatic cell mitosis in animals. There, the minus ends of microtubules nucleate on centrosomes with  $\gamma$ -tubulin, and the plus ends of microtubules are captured and then bound to the kinetochores (Kirschner and Mitchinson, 1986). However, the polarity of the forming microtubules and the location of microtubule ends with respect to the kinetochores have not been well established for chromatin-mediated spindle formation in acentrosomal cells (Karpen and Endow, 1998). Whatever the case, after the chromatin-promoted nucleation and polymerization of microtubules, perhaps the polarity of microtubules is changed through the sorting and focusing of microtubule ends by microtubule motor proteins (Heald et al., 1996).

Furthermore,  $\gamma$ -tubulin should be considered to play a role not only in microtubule nucleation but also in microtubule organization. By comparing plant and animal extracts, we found that  $\gamma$ -tubulin is much more abundant in plant cells than animal cells, perhaps as a result of the dispersed nature of plant MTOCs.  $\gamma$ -Tubulin might act as the minus end microtubule caps and may stabilize microtubules severed from multiple MTOCs. Accumulating data support the idea that  $\gamma$ -tubulin could participate in microtubule stabilization.  $\gamma$ -Tubulin has been found with the stable kinetochore microtubules that are resistant to antimicrotubular drugs in plants (Liu et al., 1995; Binarová et al., 1998a) and with the cold-stable fraction of microtubules in animal cells (Wolf and Joshi, 1996; Detraves et al., 1997).  $\gamma$ -Tubulin mutants of yeast also have enabled investigators to separate the nucleation role of  $\gamma$ -tubulin from its function in microtubule organization and dynamics (J. Paluh, personal communication). Accordingly,  $\gamma$ -tubulin in plant kinetochores could have a stabilizing effect on kinetochore–microtubule interaction and thus could play a role in microtubule capture during the spindle formation and in the regulation of microtubule dynamics at the kinetochore.

In summary, we show that plant  $\gamma$ -tubulin is present not

**(B)** DNA labeling of sorted nuclei during  $G_1$  and  $G_2$  stages of the cell cycle.

**(C)** Protein gel blot analysis of  $\gamma$ -tubulin in nuclei during  $G_1$  (lanes 1 and 3) and  $G_2$  (lanes 2 and 4) stages of the cell cycle. Coomassie blue staining of total nuclear proteins (lanes 1 and 2) is shown as well as immunostaining of  $\gamma$ -tubulin (lanes 3 and 4). Proteins from 200,000 nuclei were loaded per lane. Positions of molecular mass standards are marked at left with horizontal lines (from top to bottom: 94, 67, 43, 30, and 20 kD).

**(D)** Protein gel blot analysis of  $\gamma$ -tubulin in supernatants of cell extracts from a synchronous cell population in  $G_1$  (lanes 1 and 3) and  $G_2$  (lanes 2 and 4) stages of the cell cycle. Lanes 1 and 2 show Coomassie blue staining; immunostaining is shown in lanes 3 and 4. Ten micrograms of protein was loaded per lane. Positions of molecular mass standards are marked at left with horizontal lines (from top to bottom: 205, 116, 97, 66, and 45 kD).

only on the microtubular structures and in the cytoplasm but also in the nuclei, in which it is bound mainly to the kinetochore regions of chromosomes. In addition to its accepted nucleation role, perhaps the high abundance, different forms, and locations of  $\gamma$ -tubulin in acentriolar plant cells make it important also in microtubule dynamics and organization.

## METHODS

### Cells

*Vicia faba* seeds were germinated at 25°C in Hoagland's nutrient solution, and root meristems (1 to 2 mm long) were collected and used for immunofluorescence and biochemical analyses (asynchronous cells). In some experiments, root tip cells were synchronized by using hydroxyurea, as described by Doležel et al. (1992). The extent of cell cycle and mitotic synchrony was monitored by DNA flow cytometry and microscopically on Feulgen-stained squash preparations. Root meristems were collected at different stages of the cell cycle. In some cases, roots were treated with roscovitine (6-benzylamino-2-[*R*]-[1-hydroxymethylpropylamino]-9-isopropylpurine), a specific inhibitor of cyclin-dependent kinases (Havlíček et al., 1997) or with the antimicrotubule drugs amiprofos-methyl (APM; Mobay Co., Kansas City, KS) and taxol (Sigma). These three reagents were prepared as 20 mM stock solutions in pure dimethyl sulfoxide and diluted to working dilutions of 50, 2.5, and 1  $\mu$ M, respectively. Roots were treated for 6 hr and then processed for immunolabeling.

### Antibodies

$\gamma$ -Tubulin was detected with mouse monoclonal antibodies TU-30 (IgG<sub>2b</sub>), TU-31 (IgG<sub>2b</sub>), and TU-32 (IgG<sub>1</sub>) (Nováková et al., 1996). The antibodies were prepared against the conserved 16-amino acid peptide EYHAATRPDYISWGQTQ corresponding to the human  $\gamma$ -tubulin sequence 434 to 449 (Zheng et al., 1991). The mouse monoclonal antibody GTU-88, raised against the human  $\gamma$ -tubulin sequence from positions 38 to 53 (EEFATEGTDRKDVFFYN; Zheng et al., 1991), and a polyclonal antibody against  $\gamma$ -tubulin were purchased from Sigma. The tubulin subunits were detected with the mouse monoclonal antibody DM1A (IgG<sub>1</sub>), which was raised against  $\alpha$ -tubulin, or with the monoclonal antibody TUB2.1 (IgG<sub>1</sub>) raised against  $\beta$ -tubulin (both from Sigma). Alternatively, a rabbit affinity-purified antibody against the  $\alpha\beta$ -tubulin heterodimer was used (Dráber et al., 1991). The MPM2 monoclonal antibody (IgG<sub>1</sub>) raised against phosphorylated epitopes of mitotic cells (Davis et al., 1983) was kindly provided by P. Rao (University of Texas, Houston). Nucleolin was detected by an affinity-purified rabbit antibody (Bögge et al., 1996). Fluorescein isothiocyanate and indocarbocyanate (Cy3)-conjugated anti-mouse and anti-rabbit antibodies were obtained from Sigma. The anti-mouse Ig antibody conjugated with alkaline phosphatase was purchased from Promega.

### Preparation of Cell Extracts

Crude cell extracts were prepared from root tips (cut on ice and weighed) by freezing the tissues in liquid nitrogen, grinding to a fine

powder, and suspending the powder in 1 volume of the extraction buffer (50 mM K-Hepes, pH 7.4, 1 mM EGTA, 1 mM EDTA, 75 mM KCl, and 0.05% Nonidet P-40) supplemented with the protease inhibitors phenylmethylsulfonyl fluoride (1 mM) and leupeptin, aprotinin, antipain, and pepstatin (each at 10  $\mu$ g mL<sup>-1</sup>). To prepare the supernatant for the characterization of protein complexes, we centrifuged crude extracts at 30,000g for 30 min at 4°C. In some cases, the supernatant was centrifuged again at 100,000g for 10 min at 4°C.

### Cellular Fractionation and Isolation of Nuclei and Chromosomes

Nuclei were isolated by a modified procedure proposed by Doležel et al. (1992). Root meristems were chopped up in LB01 buffer (20 mM Tris-HCl, pH 7.5, 1 mM EDTA, 1 mM EGTA, 0.5 mM spermine, 80 mM KCl, 20 mM NaCl, 0.1% Triton X-100, and 15 mM  $\beta$ -mercaptoethanol, supplemented with protease inhibitors, as was the extraction buffer). The suspension was filtered through a 50- $\mu$ m (pore size) nylon mesh to remove large tissue fragments, loaded on a sucrose gradient (50, 30, and 10% of sucrose in LB01), and centrifuged at 400g for 15 min at 4°C. The 50% sucrose layer, which contained the nuclei, was centrifuged at 3000g for 10 min at 4°C. The pelleted nuclei were used for immunoblotting either directly or after treatment with DNase or extractions with various buffers. Routinely, ~200,000 nuclei were isolated from 20 root tips.

The upper layer of the cytoplasm from the sucrose gradient was collected and clarified by centrifugation at 30,000g for 30 min (4°C) and processed for immunoblotting.

Metaphase chromosomes were isolated from hydroxyurea-synchronized root meristem cells that were accumulated at metaphase with use of APM, as described by Doležel et al. (1992).

### Sorting of Nuclei

The suspension of isolated nuclei was stained with 4',6-diamidino-2-phenylindole (DAPI; 2  $\mu$ g mL<sup>-1</sup>). Flow-cytometric analysis and sorting were performed with a FACS Vantage flow cytometer (Becton Dickinson, San Jose, CA) equipped with an Innova 305C laser (Coherent, Santa Clara, CA) tuned to multiline UV light (333.6 to 363.8 nm). The fluorescence pulse area (FL-A) of the nuclei was analyzed, and the sorting window was set on a dot plot of FL-A and fluorescence pulse width (FL-W; Figure 4A). For electrophoresis, 200,000 nuclei were sorted into a tube containing 500  $\mu$ L of LB01 buffer supplemented with protease inhibitors. For microscopic observation, 5000 nuclei were sorted into a 15- $\mu$ L drop of LB01 buffer containing 10% sucrose and placed on a microscopic slide.

### Treatment of Isolated Nuclei

Isolated nuclei were washed twice in DNase buffer (20 mM Tris-HCl, pH 7.8, 2 mM EGTA, 25 mM MgCl<sub>2</sub>, plus protease inhibitors as described for extraction buffer) and pelleted by centrifugation (1000g for 10 min). The nuclei were digested for 1 hr at 37°C with 300  $\mu$ g mL<sup>-1</sup> DNase I (Boehringer Mannheim) in DNase buffer. Control nuclei were incubated under identical conditions in DNase buffer without the enzyme. Digested nuclei were pelleted at 1000g for 10 min, and the supernatant and pelleted nuclei were analyzed by immunoblotting. Alternatively, isolated nuclei were extracted in modified LB01 buffer (20 mM Tris-HCl, pH 7.5, 1 mM EDTA, 1 mM EGTA, 0.5 mM

spermin, and 10% sucrose plus protease inhibitors, as for the extraction buffer) supplemented with various concentrations of NaCl (75, 200, 300, and 500 mM). In some cases, the buffer was supplemented with one of the following components: 0.5 M KI, 4 M urea, or 0.5% deoxycholate plus 0.1% SDS. After a 15-min extraction at 4°C, nuclei were pelleted at 1000g for 10 min, and the supernatant and nuclei were analyzed by immunoblotting.

### Electrophoresis and Immunoblot Analysis

Proteins separated by SDS-PAGE on 7.5 or 10% polyacrylamide gels were stained by Coomassie Brilliant Blue R 250 (Serva, Heidelberg, Germany) or were electrophoretically transferred to a polyvinylidene difluoride membrane. Details of the procedure for immunostaining by using a secondary antibody labeled with alkaline phosphatase are described elsewhere (Dráber et al., 1989). Antibodies TU-30, TU-31, and TU-32 were used as undiluted supernatants. Antibodies GTU-38, DM1A, and TUB2 were diluted 1:1000.

### Immunofluorescence

Root tips were fixed for 1 hr in 3.7% paraformaldehyde, digested, and squashed, as described by Binarová et al. (1993). Thereafter, the cells were postfixed for 10 min in methanol at  $-20^{\circ}\text{C}$ , rehydrated in PBS, and processed for immunostaining. Isolated chromosomes or nuclei attached to poly-L-lysine-coated slides also were fixed for 10 min in methanol at  $-20^{\circ}\text{C}$  and processed for immunostaining. Antibodies TU-30, TU-31, and TU-32 were used as undiluted supernatants; antibodies DM1A, TUB2.1, and MPM2 were diluted 1:500. Rabbit affinity-purified antibody against  $\gamma$ -tubulin and rabbit affinity-purified antibody against  $\alpha\beta$ -tubulin heterodimer were used at dilutions of 1:5 and 1:10, respectively. For double-labeled immunofluorescence with rabbit antibodies and mouse monoclonal antibodies, slides first were incubated with the polyclonal antibody, washed, and incubated with the monoclonal antibody. Samples then were incubated simultaneously with a mixture of fluorescein isothiocyanate- and Cy3-conjugated secondary antibodies diluted 1:50 and 1:400, respectively. DAPI staining of DNA, mounting of slides, and observation proceeded as described earlier by Binarová et al. (1993). Slides were examined with a microscope (model BX 60; Olympus Optical [Europa] GmbH, Hamburg, Germany) equipped with a  $100\times 1.4$  oil immersion objective, epi-illumination, and a 35-mm (focal length) camera or, alternatively, with a confocal laser scanning microscope invert (model LSM 410; Zeiss, Jena, Germany) equipped with an He/Ne laser (543 nm) and a UV light laser (351/364 nm) (Enterprise II; Coherent, Auburn, CA). Pinholes were adjusted to obtain thin optical sections ( $\sim 1.0\ \mu\text{m}$  thick). Z-series of cells were taken by optical sectioning at a distance of  $1\ \mu\text{m}$ . Using the three-dimensional software of the confocal laser scanning microscope, we obtained 500 galleries and performed three-dimensional reconstructions.

### ACKNOWLEDGMENTS

We thank Jarmila Čihalíková, Jan Vrána, and Vadym Sulimenko for assistance with nuclei isolation, flow cytometric analysis, and sorting and densitometry. We are grateful to Miloslava Mazurová and Jitka Weiserová for excellent technical assistance. Gifts of antibody

MPM2 from Prof. Potu Rao (University of Texas, Houston) and a sample of amiprofos-methyl from the Agricultural Chemical Division of the Mobay Corp. (Kansas City, MO) are gratefully acknowledged. This work was supported by Grant No. A5020803/1998 from the Grant Agency of the Czech Academy of Sciences and Grant Nos. 204/98/1054 and 521/96/K117 from the Grant Agency of the Czech Republic.

Received September 27, 1999; accepted January 4, 2000.

### REFERENCES

- Akashi, T., Yoon, Y., and Oakley, B.R. (1997). Characterization of  $\gamma$ -tubulin complexes in *Aspergillus nidulans* and detection of putative  $\gamma$ -tubulin interacting proteins. *Cell Motil. Cytoskeleton* **37**, 149–158.
- Bajer, A.S., and Mole-Bajer, J.M. (1986). Reorganization of microtubules in endosperm cells and cell fragments of the higher plant *Haemanthus* in vivo. *J. Cell Biol.* **102**, 263–281.
- Bajer, A., and Ostergen, G. (1961). Centromere-like behaviour of non-centromeric bodies. I. Neo-centric activity in chromosome arms at mitosis. *Hereditas* **47**, 563–598.
- Binarová, P., Cihalíková, J., and Doležel, J. (1993). Localization of MPM-2 recognized phosphoproteins and tubulin during cell cycle progression in synchronized *Vicia faba* root meristem cells. *Cell Biol. Int.* **9**, 847–856.
- Binarová, P., Hause, B., Doležel, J., and Dráber, P. (1998a). Association of  $\gamma$ -tubulin with kinetochores in *Vicia faba* meristem cells. *Plant J.* **14**, 751–757.
- Binarová, P., Doležel, J., Heberle-Bors, E., Dráber, P., Strnad, M., and Bögre, L. (1998b). Treatment of *Vicia faba* root tip cells with specific inhibitors to cyclin-dependent kinase leads to abnormal spindle formation. *Plant J.* **16**, 697–707.
- Bögre, L., Jonak, C., Mink, M., Meskiene, I., Traas, J., Ha, D.T.C., Swoboda, I., Plank, C., Wagner, E., Heberle-Bors, E., and Hirt, H. (1996). Developmental and cell cycle regulation of alfalfa *nucM1*, a plant homolog of the yeast Nsr1 and mammalian nucleolin. *Plant Cell* **8**, 417–428.
- Bonnacorsi, S., Giansanti, M.G., and Gatti, M. (1998). Spindle self-organization and cytokinesis during male meiosis in *asterless* mutants of *Drosophila melanogaster*. *J. Cell Biol.* **142**, 751–761.
- Brunet, S., Polanski, Z., Verlhac, M.H., Kubiak, J., and Maro, B. (1998). Bipolar meiotic spindle formation without chromatin. *Curr. Biol.* **8**, 1231–1234.
- Chan, A., and Cande, W.Z. (1998). Maize meiotic spindles assemble around chromatin and do not require paired chromosomes. *J. Cell Sci.* **111**, 3508–3515.
- Curtenaz, S., Wright, M., and Hackman, K. (1997). Localization of  $\gamma$ -tubulin in the mitotic and meiotic nuclei of *Euplotes octocarinatus*. *Eur. J. Protistol.* **33**, 1–12.
- Davis, F.M., Tsao, T.Y., Fowler, S.K., and Rao, P.N. (1983). Monoclonal antibodies to mitotic cells. *Proc. Natl. Acad. Sci. USA* **80**, 2926–2930.
- Dawe, R.K., Reed, L.M., Yu, H., Muszynski, M.G., and Hiatt, E.N.



- (1999). A maize homolog of mammalian CENPC is a constitutive component of the inner kinetochore. *Plant Cell* **11**, 1227–1238.
- De Saint Phalle, B., and Sullivan, W.** (1998). Spindle assembly and mitosis without centrosomes in parthenogenetic *Sciara* embryos. *J. Cell Biol.* **141**, 1383–1391.
- Detraves, C., Mazarguil, H., Lajoie-Mazenc, I., Julian, M., Raynaud-Messina, B., and Wright, M.** (1997). Protein complexes containing  $\gamma$ -tubulin are present in mammalian brain microtubule protein preparations. *Cell Motil. Cytoskeleton* **36**, 179–189.
- Doležel, J., Ciháliková, J., and Lucretti, S.** (1992). A high-yield procedure for isolation of metaphase chromosomes from root tips of *Vicia faba* L. *Planta* **188**, 93–98.
- Dráber, P., Dráberová, E., Linhartová, I., and Viklický, V.** (1989). Differences in the exposure of C- and N-terminal tubulin domains in cytoplasmic microtubules detected with domain-specific monoclonal antibodies. *J. Cell Sci.* **92**, 519–528.
- Dráber, P., Dráberová, E., and Viklický, V.** (1991). Immunostaining of human spermatozoa with tubulin domain-specific monoclonal antibodies. Recognition of a unique epitope in the sperm head. *Histochemistry* **195**, 519–524.
- Havlíček, L., Hanuš, J., Veselý, J., Leclerc, S., Meijer, L., Shaw, G., and Strnad, M.** (1997). Cytokinin-derived cyclin-dependent kinase inhibitors: Synthesis and cdc2 inhibitory activity of olomoucine and related compounds. *J. Med. Chem.* **40**, 408–412.
- Heald, R., Tournebize, C., Blank, T., Sandantzopoulos, R., Becker, P., Hyman, A.R., and Karsenti, E.** (1996). Self-organization of microtubules into bipolar spindles around artificial chromosomes in *Xenopus* egg extracts. *Nature* **385**, 420–425.
- Heald, R., Tournebize, C., Habermann, A., Karsenti, E., and Hyman, A.** (1997). Spindle assembly in *Xenopus* egg extracts: Respective role of centrosomes and microtubule self-organization. *J. Cell Biol.* **138**, 615–628.
- Houben, A., Guttenbach, W., Kres, W., Pich, U., Schubert, I., and Schmid, M.** (1995). Immunostaining and interphase arrangement of field bean kinetochores. *Chromosoma Res.* **3**, 27–31.
- Hyman, A., and Karsenti, E.** (1998). The role of nucleation in patterning microtubule networks. *J. Cell Sci.* **111**, 2077–2083.
- Jeng, R., and Sterns, T.** (1999).  $\gamma$ -Tubulin complexes: Size does matter. *Trends Cell Biol.* **9**, 339–342.
- Joshi, H.C., and Palevitz, B.A.** (1996).  $\gamma$ -Tubulin and microtubule organization in plants. *Trends Cell Biol.* **6**, 41–44.
- Joshi, H.C., McNamara, L., and Cleveland, D.W.** (1992).  $\gamma$ -Tubulin is a centrosomal protein required for cell cycle-dependent microtubule nucleation. *Nature* **356**, 80–83.
- Karpen, G.H., and Endow, S.A.** (1998). Meiosis: Chromosome behaviour and spindle dynamics. In *Dynamics of Cell Division*, S.A. Endow and D.M. Glover, eds (Oxford, UK: Oxford University Press), pp. 205–247.
- Kirschner, M., and Mitchinson, T.** (1986). Beyond self assembly: From microtubules to morphogenesis. *Cell* **45**, 329–342.
- Knop, M., and Schiebel, E.** (1997). Spc98p and Spc97p of the yeast  $\gamma$ -tubulin complex mediate binding to the spindle pole body via their interaction with Spc110p. *EMBO J.* **16**, 6985–6995.
- Kube-Granderath, E., and Schliwa, M.** (1997). Unusual distribution of  $\gamma$ -tubulin in the giant fresh water amoeba *Reticulomyxa filosa*. *Eur. J. Cell Biol.* **72**, 287–296.
- Liu, B., Marc, J., Joshi, H.C., and Palevitz, B.A.** (1993).  $\gamma$ -Tubulin-related protein associated with microtubule arrays of higher plants in cell cycle-dependent manner. *J. Cell Sci.* **104**, 1217–1228.
- Liu, B., Joshi, H.C., and Palevitz, B.A.** (1995). Experimental manipulation of  $\gamma$ -tubulin distribution in Arabidopsis using anti-microtubule drugs. *Cell Motil. Cytoskeleton* **31**, 113–129.
- Mazia, D.** (1984). Centrosomes and mitotic poles. *Exp. Cell Res.* **153**, 1–15.
- McDonald, A.R., Liu, B., Joshi, H.C., and Palevitz, B.A.** (1993).  $\gamma$ -Tubulin is associated with cortical-microtubule organizing zone in the developing guard cells of *Allium cepa* L. *Planta* **191**, 357–361.
- Moritz, M., Zheng, Y., Alberts, B.M., and Oegema, K.** (1998). Recruitment of the  $\gamma$ -tubulin complex to *Drosophila* salt-stripped centrosome scaffolds. *J. Cell Biol.* **142**, 775–786.
- Moudjou, M., Bordes, N., Paintrand, M., and Bornens, M.** (1996).  $\gamma$ -Tubulin in mammalian cells: The centrosomal and cytosolic forms. *J. Cell Sci.* **109**, 875–887.
- Nováková, M., Dráberová, E., Schurman, W., Czihak, G., Viklický, V., and Dráber, P.** (1996).  $\gamma$ -Tubulin redistribution in taxol-treated mitotic cells probed by monoclonal antibodies. *Cell Motil. Cytoskeleton* **33**, 38–51.
- Oakley, B.R., Oakley, E., Yoon, Y., and Jung, M.K.** (1990).  $\gamma$ -Tubulin is a component of the spindle pole body that is essential for microtubule function in *Aspergillus nidulans*. *Cell* **61**, 1289–1301.
- Oegema, K., Wiese, C., Martin, O.C., Miligan, R.A., Iwamatsu, A., Mitchinson, T.J., and Zheng, Y.** (1999). Characterization of two related *Drosophila*  $\gamma$ -tubulin complexes that differ in their ability to nucleate microtubules. *J. Cell Biol.* **144**, 721–733.
- Palevitz, B.A.** (1993). Morphological plasticity of the mitotic apparatus in plants and its developmental consequences. *Plant Cell* **5**, 1001–1009.
- Pereira, G., Knop, M., and Schiebel, E.** (1998). Spc98 directs the yeast  $\gamma$ -tubulin complex into the nucleus and is subject to cell cycle-dependent phosphorylation on the nuclear site of the spindle body. *Mol. Biol. Cell* **9**, 775–793.
- Smertenko, A., Blume, Y., Viklický, V., and Dráber, P.** (1997). Exposure of tubulin structural domains in *Nicotiana tabacum* microtubules probed by monoclonal antibodies. *Eur. J. Cell Biol.* **72**, 104–112.
- Smirnova, E.A., and Bajer, A.S.** (1998). Early stages of spindle formation and independence of chromosome and microtubule cycles in *Haemantus endosperm*. *Cell Motil. Cytoskeleton* **40**, 22–37.
- Stearns, T., and Kirschner, M.W.** (1994). In vitro reconstitution of centrosome assembly and function: The central role of  $\gamma$ -tubulin. *Cell* **76**, 623–637.
- Stoppin, V., Lambert, A.M., and Vantard, M.** (1996). Plant microtubule-associated proteins (MAPs) affect microtubule nucleation and growth at the plant nuclei and mammalian centrosomes. *Eur. J. Cell Biol.* **69**, 11–23.
- Stoppin-Mellet, V., Petr, C., Buendia, B., Karsenti, E., and Lambert, A.** (1999). Tobacco BY-2 cell-free extracts induce the recovery of microtubule nucleating activity of inactivated mammalian centrosomes. *Biochim. Biophys. Acta* **1449**, 101–106.
- Sullivan, K.F.** (1998). A moveable feast: The centromere-kinetochore complex in cell division. In *Dynamics of Cell Division*, S.A.

- Endow and D.M. Glover, eds (Oxford, UK: Oxford University Press), pp. 123–165.
- Vorobjev, I.A., Svitkina, T.M., and Borisy, G.** (1997). Cytoplasmic assembly of microtubules in cultured cells. *J. Cell Sci.* **110**, 2635–2645.
- Wolf, K.W., and Joshi, H.C.** (1996). Microtubule organization and distribution of  $\gamma$ -tubulin in male meiosis of Lepidoptera. *Mol. Reprod. Dev.* **45**, 547–549.
- Yu, H., Muszynski, M.G., and Dawe, K.R.** (1999). The maize homologue of the cell cycle checkpoint MAD2 reveals kinetochore substructure and contrasting mitotic and meiotic localization patterns. *J. Cell Biol.* **145**, 425–435.
- Yvon, A.M., and Wadsworth, P.** (1997). Non-centrosomal microtubule formation and measurement of minus end microtubule dynamics in A498 cells. *J. Cell Sci.* **110**, 2391–2401.
- Zhang, D., and Nicklas, R.B.** (1995). The impact of chromosomes and centrosomes on spindle assembly as observed in living cells. *J. Cell Biol.* **129**, 1287–1300.
- Zheng, Y., Jung, M.K., and Oakley, B.R.** (1991).  $\gamma$ -Tubulin is present in *Drosophila melanogaster* and *Homo sapiens* and is associated with centrosome. *Cell* **65**, 817–823.
- Zheng, Y., Wong, M.L., and Mitchinson, T.** (1995). Nucleation of microtubule assembly by a  $\gamma$ -tubulin-containing ring complex. *Nature* **378**, 578–583.

## Nuclear $\gamma$ -Tubulin during Acentriolar Plant Mitosis

Pavla Binarová, Vera Cenklová, Bettina Hause, Elena Kubátová, Martin Lysák, Jaroslav Dolezel, László Bögre and Pavel Dráber  
*Plant Cell* 2000;12;433-442  
DOI 10.1105/tpc.12.3.433

This information is current as of June 13, 2012

<b>References</b>	This article cites 48 articles, 19 of which can be accessed free at: <a href="http://www.plantcell.org/content/12/3/433.full.html#ref-list-1">http://www.plantcell.org/content/12/3/433.full.html#ref-list-1</a>
<b>Permissions</b>	<a href="https://www.copyright.com/ccc/openurl.do?sid=pd_hw1532298X&amp;issn=1532298X&amp;WT.mc_id=pd_hw1532298X">https://www.copyright.com/ccc/openurl.do?sid=pd_hw1532298X&amp;issn=1532298X&amp;WT.mc_id=pd_hw1532298X</a>
<b>eTOCs</b>	Sign up for eTOCs at: <a href="http://www.plantcell.org/cgi/alerts/ctmain">http://www.plantcell.org/cgi/alerts/ctmain</a>
<b>CiteTrack Alerts</b>	Sign up for CiteTrack Alerts at: <a href="http://www.plantcell.org/cgi/alerts/ctmain">http://www.plantcell.org/cgi/alerts/ctmain</a>
<b>Subscription Information</b>	Subscription Information for <i>The Plant Cell</i> and <i>Plant Physiology</i> is available at: <a href="http://www.aspb.org/publications/subscriptions.cfm">http://www.aspb.org/publications/subscriptions.cfm</a>